Multi-harmonic generator based on the synchronization of a nonlinear bipolar oscillator

Elena de Cos, Franco Ramírez, and Almudena Suárez, *Senior Member, IEEE*

Departamento de Ingeniería de Comunicaciones. Universidad de Cantabria. Av. Los Castros s/n 39005 Santander. Spain. almu@dicom.unican.es

Abstract **— A multi-harmonic generator, based on the synchronization of a bipolar oscillator at the fundamental frequency is presented. The fact that the oscillator generates, by itself, the high harmonic content reduces the requirements of RF input power. The first-harmonic injection enables relatively large synchronization band. The design is based on a bipolar transistor oscillator, spending a long fraction of its period in saturated regime. The circuit is simulated through harmonic balance, performing stability and phase-noise analyses. The possibility of frequency conversion between different harmonic components of the oscillator has also been evaluated. A prototype providing harmonics between 0.24 and 2.4 GHz has been manufactured, with very good agreement with the experimental results.**

I. INTRODUCTION

Frequency-multiplication [1] or frequency-division functions [2] can be achieved from the sub-harmonic or harmonic synchronization of an oscillator, which constitutes a natural mechanism for frequency synthesis. If the original oscillator has a rich harmonic content, without great power unbalance between the different spectral lines, the fundamental-harmonic synchronization to an external source provides multi-harmonic generation with low input-power requirements. Multi-harmonic generators delivering harmonic frequencies with phase relationship are used, for instance, in measurement systems dealing with non-sinusoidal waveforms [3]. In previous works [3-5], this multi-harmonic generation has been based on the employment of Schottky diodes, step-recovery diodes or, more recently, nonlinear transmission lines. The resulting circuit usually requires high input power to lead the device (or devices) to the nonlinear regime that enables the harmonic generation. In comparison, the oscillator synchronization allows a design based on transistor technology, with a reduced number of devices, which is an advantage for integration and low power consumption. The circuit will operate from low input-power values, since the harmonic components are not the result of the action of the active device on the input signal, but generated by the oscillator itself.

The fundamental frequency injection should enable relatively large synchronization bandwidth, with the phase noise at low frequency offsets from the carrier being mainly determined by the input generator, increasing as *20·log(N)* with the order of the harmonic component Nf_0. The oscillating nature of the system should allow other forms of frequency conversion. Actually, for input frequency close to the harmonic component Mf_0, the synchronization of the multi-harmonic oscillator would provide the frequency components Nf_0/M.

Using these principles, a bipolar based oscillator for multi-harmonic generation has been designed here. For reasons of transistor availability and manufacturing simplicity, a 0.24 GHz to 2.4 GHz prototype has been designed and experimentally characterized, obtaining very good agreement with the harmonic-balance simulations.

II. OSCILLATOR FOR MULTI-HARMONIC GENERATION

The initial free-running oscillator circuit is designed using a bipolar transistor (Fig. 1). It is similar to a Colpitt's oscillator, although the connection of the input RF generator requires a resistance at the base terminal. The output signal is taken at the collector terminal through a high-input impedance amplifier. The operation of the circuit can be described with the following simplified equations:

$$\frac{dv_{CB}}{dt} = -\frac{i_C}{C_1} + i_L\left(\frac{1}{C_1}+\frac{1}{C_2}\right) - \frac{V_{BB}}{C_2R_E} + \frac{v_{BE}}{C_2R_E} + \frac{i_B}{C_2} \quad \text{(a)}$$

$$\frac{di_L}{dt} = \frac{V_{CC}-V_{BB}}{L} - \frac{v_{CB}}{L} - \frac{R_c}{L}i_L \quad \text{(b)} \qquad (1)$$

$$\frac{dv_{BE}}{dt} = \frac{V_{BB}}{C_2R_E} - \frac{v_{BE}}{C_2R_E} - \frac{i_B}{C_2} - \frac{i_L}{C_2} \quad \text{(c)}$$

A relatively big value of the inductor L is selected, such that its associated time constant L/R_C gives rise to a slow current increase. This makes the transistor operate in saturated conditions ($v_{CB}<0$) during a long fraction of the period. Fig. 2 shows the waveforms, at different nodes of

0-7803-7695-1/03/$17.00 © 2003 IEEE

the circuit. These waveforms were obtained through HB with 15 harmonic components taking the parasitics in the linear and non-linear elements into account. The nearly zero v_{CE} voltage prevents the current flow through C_1 and therefore $i_C \cong i_L$. As gathered from (1.a), the voltage v_{CB} grows with i_L, until a value is reached for which v_{CB} becomes positive and the transistor switches to the active mode. The voltage v_{CB} increases as long as the right-hand term of (1.a) has positive sign. But the i_L current decreases with v_{CB} (1.b). At a time value close to that for which the sign of i_L changes, the v_{CB} voltage starts to decrease, until it becomes negative again, which determines the transition to the saturated state.

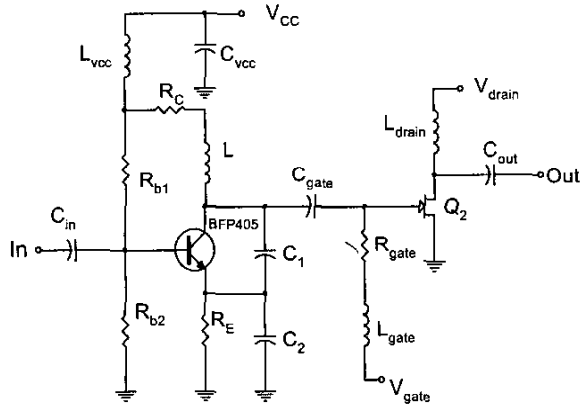

Fig. 1. Schematic of the fundamentally synchronized oscillator for multi-harmonic generation.

The employment of an auxiliary generator (AG) [2], operating at the oscillation frequency $\omega_{AG}=\omega_0$ in the HB design, enables setting this frequency to the desired value ω_0. Here, f_0=0.24 GHz has been chosen. The inductance L and the AG amplitude are optimized, for each C_2 value, so as to fulfil the AG non-perturbation condition. This condition is given by the zero value of its associated admittance function (current to voltage relationship). In this way it is possible to tune C_2 for a reduction, in the v_{CE} voltage, of the fraction of the cycle with non-zero value. The final percentage of this cycle is about 20% of the period. The frequency scalability of the circuit has also been analyzed. This is possible, since the harmonic generation relies on the switching of the transistor between saturation and forward active operation. A ten times higher fundamental frequency, 2.4 GHz, requires the values L=1.25nH and C_2=4 pF, together with a reduction of the resistances.

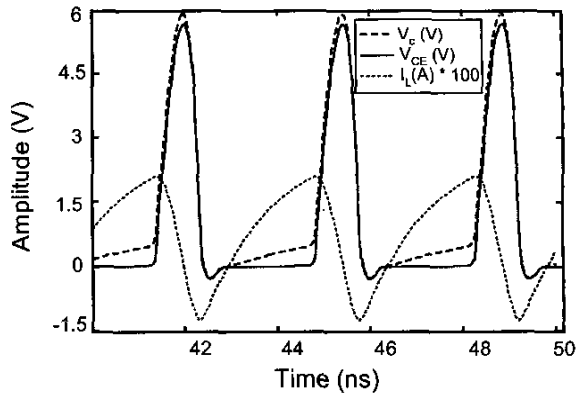

Fig. 2. Operation of the bipolar-based oscillator. The transistor switches between saturated and active modes.

III. MULTI-HARMONIC GENERATOR

Once the free-running oscillator has been designed, the next step is the introduction of an RF input signal. When this signal synchronizes to the first harmonic component of the self-oscillation, the oscillation harmonics become multiples of the input frequency. The experimental spectrum for input frequency f_{in}= 0.24 GHz and input power P_{in}=-16 dBm is shown in Fig. 3a. The DC collector current is I_C=65 mA and the power consumption is 500 mW. For a better insight into the frequency generation capabilities of the circuit, the measurements have been carried out for a prototype without an output amplifier. The output amplifier should provide 20 dB gain. As can be seen, the harmonic components N=4 to N=8 have similar power levels. For the selection of a particular harmonic component of order N, the neighbouring spectral lines N-1 and N+1 can be eliminated through open-circuited $\lambda/4$ microstrip lines [4], which relaxes the specifications of the filter about Nf_{in}. This application has been experimentally tested, Fig. 3b shows the measured spectrum about the 10^{th} harmonic component.

Versus the input frequency a fundamentally synchronized oscillator provides closed solution curves that open up from a certain input power value. In the circuit we are dealing with, for the input power P_{in}=-16 dBm, an open curve is obtained at each harmonic component. This has been represented in Fig. 4., where measurements are superimposed. The limits of the synchronization band are given by two Hopf bifurcations. The experimental synchronization band (0.195 GHz to 0.365 GHz) closely agrees with the predictions. As can be seen, a relatively smooth power variation is obtained for all harmonic components.

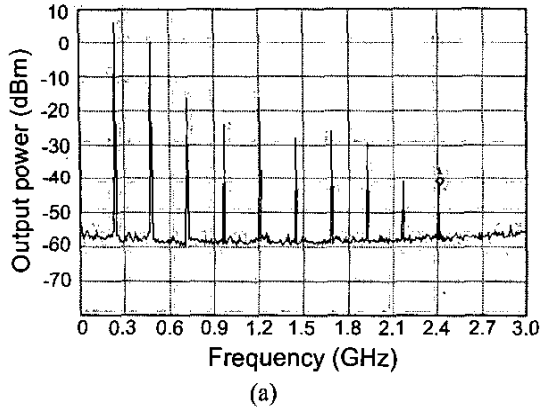

(a)

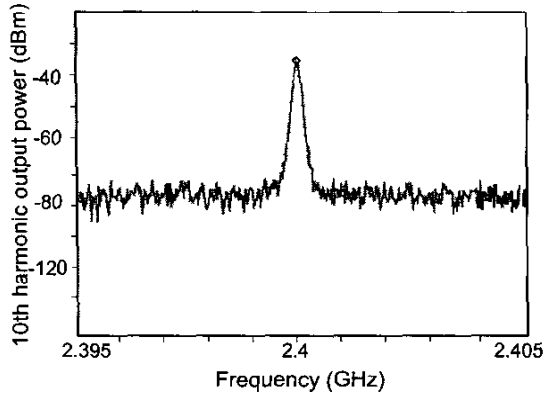

(b)

Fig. 3. (a) Output spectrum at the collector terminal (no amplification stage is used). (b) 10^{th} harmonic output power after filtering.

The linearity versus the input amplitude is analyzed in Fig. 5, where the variation of the harmonic amplitude at the orders N=7 and N=8 has been represented. Linear behavior is obtained up to P_{in}=-6 dBm, which would enable the application of the circuit in measurement systems requiring multi-harmonic generators.

As an example of other forms of operation, input-signal has been introduced about the third harmonic frequency M=3, obtaining the harmonic variation at the respective frequencies N/M=5/3f_0, N/M=6/3f_0 and N/M=7/3f_0. In this case, closed solution curves are obtained versus the input frequency (Fig. 6). They are traced through a continuation technique. The limits of the synchronization band are determined by two saddle-node bifurcations (infinite slope points of the curves). The harmonic power is similar to that obtained for fundamentally frequency injection, with a synchronization bandwidth that is also relatively large. However, the requirements in the input power are higher and increase with order M.

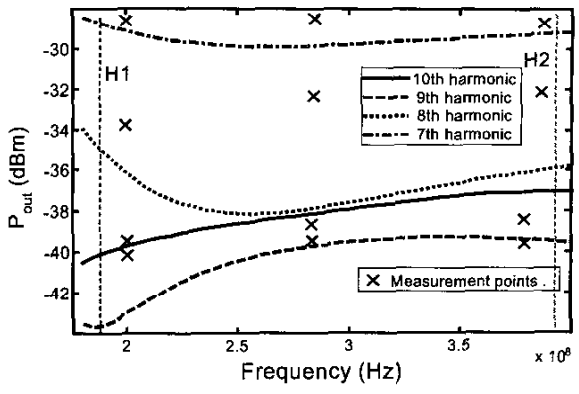

Fig. 4 Variation of the harmonic output power along the operation band.

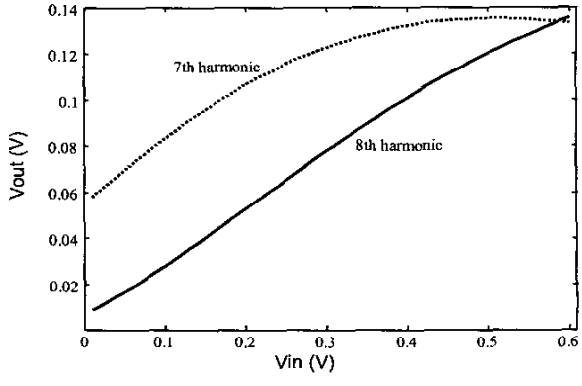

Fig. 5. Evaluation of linearity in the harmonic generation .

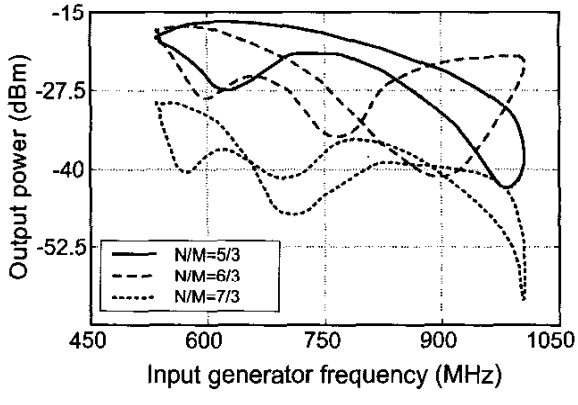

Fig. 6. Operation bands for input-signal at N=5, N=6 and N=7, for M=3.

IV. PHASE-NOISE ANALYSIS

For the phase noise analysis of the bipolar-based circuit, two current noise sources, respectively accounting for the flicker noise and the shot noise have been introduced at the transistor base terminal. The amplitude noise of the input generator has been neglected. For phase noise analysis, the conversion matrix formalism is applied [6]. The harmonic-balance equations are linearized about the nonlinear steady state, replacing the nonlinear device with its conversion matrix and obtaining the linear network matrixes at the sidebands. The resulting phase-noise spectral density, at the circuit output, is shown in Fig. 8 for the fundamental frequency and the harmonic component N=10. The results are compared with the phase noise of the input generator and that of the free-running oscillator, for which, in addition to the conversion matrix approach, the carrier modulation approach [6] has been employed.

Close to the carrier the phase noise at the fundamental frequency, of the harmonic generator approximately follows the input-oscillator noise. For the same interval of offset frequencies, the phase noise at the harmonic component N=10 is about 20 dB, higher, due to the frequency multiplication. Far from the carrier, the phase noise at the fundamental frequency approaches that of the free-running oscillator. The phase-noise level at the harmonic component N=10 keeps about 20 dB higher.

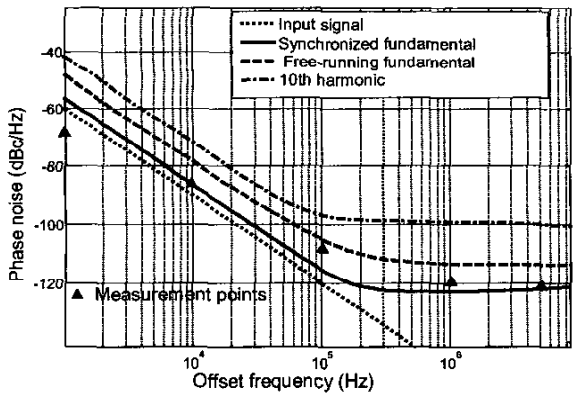

Fig. 8 Phase noise analysis of the multi-harmonic generator about the fundamental frequency and the harmonic component N=10. The results are compared with those of the free-running oscillator. Measurements have been superimposed.

V. CONCLUSION

Multi-harmonic generation has been obtained through the fundamental synchronization of an oscillator with high harmonic content. The oscillator is based on a bipolar transistor spending a long fraction of the period in saturated mode. The variation of the harmonic power along the synchronization band has been determined through harmonic balance, also evaluating the possibility of frequency conversion between different harmonic terms. The output phase noise has been calculated and compared with that of the input source. The circuit has been manufactured and measured, obtaining very good agreement with the simulation results.

ACKNOWLEDGEMENT

This work was supported by the Spanish CICYT project TIC2002-03748. The authors are grateful to Dr. Juan Mari Collantes, from the Basque Country University, for helpful discussions.

REFERENCES

[1] S. Kudszus, T. Berceli, M. Neumann, A. Tessmann, W. H. Haydl "W-band HEMT-Oscillator MMICs using subharmonic injection locking," *IEEE Trans. Microwave Theory and Techniques,* vol. 48, no. 12, Dec 2000, pp. 2526-2532.

[2] A. Suárez, J. Morales, R. Quéré, "Synchronization analysis of autonomous microwave circuits using new global stability analysis tools," *IEEE Trans. Microwave Theory and Techniques,* vol. 46, no. 5, May 1998, pp. 494-504.

[3] P. Heymann, R. Doerner, M. Rudolph, "Multiharmonic generator for relative phase calibration of nonlinear network analyzers", *IEEE trans. on Instrumentation and measurement*, vol. 50, no. 1, Feb. 2001, pp. 129-134.

[4] H. Fudem, E. C. Niehenke, "Novel millimetric wave active MMIC triplers", *IEEE MTT-S Digest*, 1998, pp. 387-390.

[5] D. Salameh, d. Linton, "Microstrip GaAs nonlinear transmission line harmonic and pulse generators", *IEEE MTT trans.* vol. 47, no. 7, Jul. 1999, pp. 1118,1121.

[6] V. Rizzoli, F. Mastri and D. Masotti, "General Noise Analysis of Nonlinear Microwave Circuits by the Piecewise Harmonic-Balance Technique", *IEEE Transactions on Microwave Theory and Techniques*, Vol. 42, No. 5, 1994, pp. 807-819.